Available online at www.sciencedirect.com
SCIENCE DIRECT
International Journal of Heat and Mass Transfer 49 (2006) 2077–2089
International Journal of HEAT and MASS TRANSFER
www.elsevier.com/locate/ijhmt

Subcooled flow boiling heat transfer and associated bubble characteristics of R-134a in a narrow annular duct

Y.M. Lie, T.F. Lin *

Department of Mechanical Engineering, National Chiao Tung University, Hsinchu, Taiwan 30010, ROC

Received 17 July 2005; received in revised form 30 November 2005
Available online 28 February 2006

Abstract

Experiments are conducted here to investigate how the channel size affects the subcooled flow boiling heat transfer and associated bubble characteristics of refrigerant R-134a in a horizontal narrow annular duct. The gap of the duct is fixed at 1.0 and 2.0 mm in this study. From the measured boiling curves, the temperature undershoot at ONB is found to be relatively significant for the subcooled flow boiling of R-134a in the duct. The R-134a subcooled flow boiling heat transfer coefficient increases with a reduction in the gap size, but decreases with an increase in the inlet liquid subcooling. Besides, raising the imposed heat flux can cause a substantial increase in the subcooled boiling heat transfer coefficient. However, the effects of the refrigerant mass flux and saturated temperature on the boiling heat transfer coefficient are small in the narrow duct. Visualization of the subcooled flow boiling processes reveals that the bubbles are suppressed to become smaller and less dense by raising the refrigerant mass flux and inlet subcooling. Moreover, raising the imposed heat flux significantly increases the bubble population, coalescence and departure frequency. The increase in the bubble departure frequency by reducing the duct size is due to the rising wall shear stress of the liquid flow, and at a high imposed heat flux many bubbles generated from the cavities on the heating surface tend to merge together to form big bubbles. Correlation for the present subcooled flow boiling heat transfer data of R-134a in the narrow annular duct is proposed. Additionally, the present data for some quantitative bubble characteristics such as the mean bubble departure diameter and frequency and the active nucleation site density are also correlated.
© 2006 Elsevier Ltd. All rights reserved.

1. Introduction

Flow boiling heat transfer in small channels has been intensively investigated in the past decade since the important role it plays in designing highly compact heat exchangers which are widely used in current energy saving air conditioning and refrigeration systems [1,2]. The use of subcooled flow boiling in these systems can further improve their energy efficiencies due to the presence of large temperature drop in the flows along with the boiling processes. Certain characteristics of flow boiling for some fluids in small circular and rectangular channels and narrow concentric ducts have been reported in literature [3–12]. These studies suggest that when the channel is smaller than certain critical size, the two-phase flow regimes and the associated heat transfer differ significantly from those in channels of conventional size. Some studies indicate that in small channels the flow boiling heat transfer is dominated by the bubble nucleation, which is ascertained by the strong dependence of the boiling heat transfer coefficient on the heat flux and weak dependence on the mass flux. While other studies show that both the bubble nucleation and convection are important in contributing the flow boiling heat transfer in small pipes. Besides, it has been noted that reducing the channel dimension produces a negative effect on the boiling heat transfer. But the opposite trend is also noted in other studies. Moreover, Sheng and Palm [13] visualized the flow pattern and bubble shape for water in a single small glass tube and noted that the bubble departure diameter depended much on the mass flow rate. Recently, Lee

* Corresponding author. Tel.: +886 35 712121x55118; fax: +886 35 726440.
E-mail address: tflin@mail.nctu.edu.tw (T.F. Lin).

0017-9310/$ - see front matter © 2006 Elsevier Ltd. All rights reserved.
doi:10.1016/j.ijheatmasstransfer.2005.11.032

Nomenclature

A_s	outside surface area of the heated inner pipe, m^2
Bo	Boiling number, $Bo = \frac{q}{G \cdot i_{fg}}$, dimensionless
D_h	hydraulic diameter, m
d_p	mean bubble departure diameter
D_p	dimensionless mean bubble departure diameter, m
f	mean bubble departure frequency, Hz
F_d	dimensionless mean bubble departure frequency
f_f	friction factor for liquid flow
Fr	Froude number, $Fr = \frac{G^2}{\rho_l^2 \cdot g \cdot D_h}$, dimensionless
g	acceleration due to gravity, m/s^2
G	mass flux, kg/m^2 s
$h_{1\phi}$	single-phase liquid convection heat transfer coefficient, W/m^2 °C
h_r	subcooled flow boiling heat transfer coefficient, W/m^2 °C
i_{fg}	enthalpy of vaporization, J/kg
Ja	Jakob number, $Ja = \frac{\rho_l \cdot C_p \cdot \Delta T_{sub}}{\rho_g \cdot i_{fg}}$, dimensionless
k_l	thermal conductivity of liquid R-134a, W/m °C
N_{ac}	active nucleation site density, n/m^2
N_{conf}	Confinement number, $N_{conf} = \frac{(\sigma/(g\Delta\rho))^{0.5}}{D_h}$, dimensionless
Nu	Nusselt number for single-phase liquid flow, $Nu = \frac{h_{1\phi} D_h}{k_l}$, dimensionless
P	system pressure, kpa
Pr_l	Prandtl number of liquid R-134a, dimensionless
q	average imposed heat flux, W/m^2
q_b, q_c, q_t	heat flux due to bubble nucleation, single-phase convection, total value, W/m^2
Q_n	net power input, W
Re_l	all liquid Reynolds number, $Re_l = \frac{GD_h}{\mu_l}$, dimensionless
T_r, $T_{r,i}$	mean, inlet temperature of liquid R-134a, °C
T_{sat}	saturated temperature of refrigerant R-134a, °C
T_w	wall temperature of heated inner pipe, °C
V_g	average volume of a departing bubble, m^3
z	axial coordinate for annular duct flow, mm

Greek symbols

ΔT	temperature difference, °C
ΔT_{sat}	wall superheat, $(T_w - T_{sat})$, °C
ΔT_{sub}	inlet subcooling, $(T_{sat} - T_{r,i})$, °C
δ	gap size of annular duct, mm
μ_l	viscosity of liquid R-134a, N s/m^2
ρ_g, ρ_l	vapor and liquid densities of R-134a, kg/m^3
$\Delta\rho$	density difference, $(\rho_l - \rho_g)$, kg/m^3
σ	surface tension, N/m

et al. [14] examined the bubble dynamics in a micro channel. The bubble departure radius was correlated by the modified form of the Levy equation.

Considerable amount of work has been carried out for subcooled flow boiling in channel of convectional size. Bang et al. [15] examined the behavior of near-wall bubbles in subcooled flow boiling of water and R-134a in a vertical rectangular channel and described the coalescence of the bubbles. The bubbles were found to be smaller at a higher mass flux. Similar study for water in a vertical annular channel conducted by Situ et al. [16] indicated that the bubble departure frequency increased with the heat flux. Results from Yin et al. [17] for R-134a in a horizontal annular duct showed that the bubble generation was suppressed by raising the refrigerant mass flux and subcooling, and only the liquid subcooling exhibited a significant effect on the bubble size. Flow boiling of FC-87 in a vertical rectangular channel investigated by Thorncroft et al. [18] manifested that both the bubble growth and departure rates increased with the Jacob number, but the bubble departure diameter decreased with the mass flux. Low pressure subcooled flow boiling inside a vertical concentric annulus examined by Zeitoun and Shoukri [19] showed that the mean size and lift duration of the bubbles increased at decreasing liquid subcooling.

The above literature review clearly indicates that extensive research has been carried out for flow boiling heat transfer of some fluids in channels of convectional size. However, the detailed bubble characteristics associated with the flow boiling in small channels remain less explored especially for new refrigerants. In a recent experimental study [20] we measured the saturated flow boiling heat transfer and associated bubble characteristics for R-134a in a horizontal narrow annular duct. In this continuing study we move further to explore the heat transfer and bubble behavior in subcooled boiling flow of R-134a in the same duct. The effects of the imposed heat flux, gap size, and R-134a mass flux and inlet subcooling on the boiling heat transfer characteristics will be examined in detail. Particularly, flow visualization is conducted here to examine the bubble characteristics associated with the flow boiling such as the mean bubble departure diameter and frequency from the heating surface, intending to improve our understanding of the subcooled flow boiling processes in a narrow channel.

2. Experimental apparatus and procedures

The experimental system employed in the previous study [20] is also used here to investigate the subcooled flow boiling of R-134a in a narrow annular duct. It is schematically depicted in Fig. 1. The experimental apparatus consists of three main loops, namely, a refrigerant loop, a water–glycol loop, and a hot-water loop. The test section of the experimental apparatus is a horizontal annular duct with the outer pipe made of Pyrex glass to permit the visualiza-

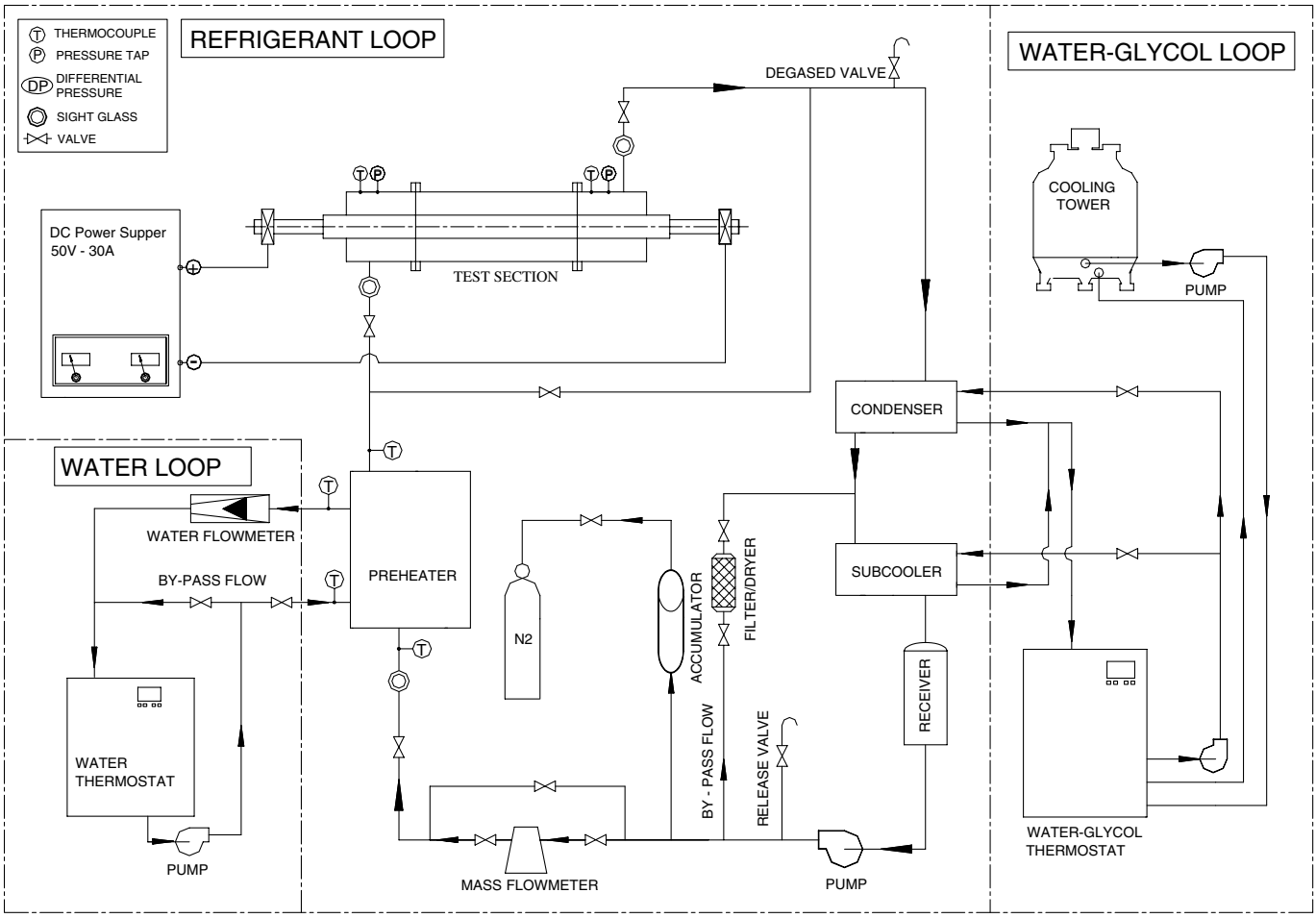

Fig. 1. Schematic of experimental system for the annular duct.

tion of boiling processes in the refrigerant flow. The glass pipe is 160 mm long with an inside diameter of 20.0 mm. Its wall is 4.0 mm thick. Both ends of the pipe are connected with copper tubes of the same size by means of flanges and are sealed by O-rings. The inner copper pipe has 16.0 or 18.0-mm nominal outside diameter with its wall being 1.5 or 2.5 mm thick and is 0.73 m long. Thus the gap of the annular duct is 2.0 or 1.0 mm ($D_h = 4.0$ or 2.0 mm). In order to insure the gap being smooth and uniform, the outside surface of the inner pipe is polished by fine sandpaper. An electric cartridge heater of 160 mm in length and 13.0 mm in diameter with a maximum power output of 800 W is inserted into the inner pipe. Then, 8 T-type calibrated thermocouples are electrically insulated by electrically nonconducting thermal bond before they are fixed on the inside surface of the inner pipe so that the voltage signals from the thermocouples are not interfered with the DC current passing through the cartridge heater. The thermocouples are positioned at three axial stations along the inner pipe. The details of the three loops, photographic apparatus, data acquisition unit, and experimental procedures are already available in our early studies [17,20] and are not repeated here.

3. Data reduction

The imposed heat flux for the subcooled boiling of the refrigerant flow in the annular duct is calculated on the basis of the total power input and the total outside heat transfer area of the inner pipe A_s. The results from the single-phase liquid convection test in the duct indicate that the heat loss from the test section is generally less than $\pm 4\%$ of the total power input. The outside surface temperature T_w of the inner heated pipe at each thermocouple location is deduced from the measured inside surface temperature of the pipe by accounting for the radial heat conduction in the pipe wall. In the two-phase test, the local subcooled flow boiling heat transfer coefficient is defined as

$$h_r = \frac{Q_n/A_s}{(T_w - T_r)} \tag{1}$$

Here T_r is the local mean liquid refrigerant temperature and is estimated by assuming that it varies linearly in the axial direction and Q_n is the net heat transfer rate to the refrigerant.

Uncertainties of the measured heat transfer coefficients are estimated according to the procedures proposed by

Table 1
Summary of the uncertainty analysis

Parameter	Uncertainty
Annular pipe geometry	
Length, width and thickness (%)	±0.5%
Area (%)	±1.0%
Parameter measurement	
Temperature, T (°C)	±0.2
Temperature difference, ΔT (°C)	±0.3
System pressure, P (kPa)	±2
Mass flux of refrigerant, G (%)	±2
Subcooled flow boiling heat transfer on inner pipe	
Imposed heat flux, q (%)	±4.5
Heat transfer coefficient, h_r (%)	±14

Kline and McClintock [21] for the propagation of errors in physical measurement. The results from this uncertainty analysis are summarized in Table 1.

4. Results and discussion

The present experiments for exploring the subcooled flow boiling heat transfer and associated bubble characteristics of refrigerant R-134a flowing in a narrow annular duct are conducted for the refrigerant mass flux G varying from 200 to 300 kg/m^2 s, imposed heat flux q from 0 to 55 kW/m^2, inlet liquid subcooling ΔT_{sub} from 6 to 13 °C, duct gap δ from 1 to 2 mm, and refrigerant saturated temperature T_{sat} from 10 to 15 °C (corresponding to the R-134a saturated pressure from 414 to 488 kPa). Attention will be focused on how the subcooled flow boiling heat transfer and associated bubble behavior are affected by the duct size and inlet liquid subcooling. To insure the repeatability of the results, the data are finalized by repeating the test four times for each case. The heat transfer characteristics in the R-134a subcooled flow boiling are demonstrated first in terms of the measured boiling curves for various flow and thermal conditions. Then, selected experimental data and flow photos from the present study are presented to illustrate the subcooled flow boiling heat transfer coefficient and associated bubble characteristics in the boiling flow including bubble departure diameter, departure frequency and active nucleation site density. Finally, empirical equations are proposed to correlate the present data for the subcooled flow boiling heat transfer coefficient and bubble characteristics.

4.1. Subcooled flow boiling curves

The effects of the three experimental parameters, namely, the refrigerant mass flux, inlet subcooling, and gap size of the duct, on the subcooled flow boiling characteristics at the middle axial location ($z = 80$ mm) of the annular duct are illustrated in Fig. 2. First, the effects of the refrigerant mass flux are shown in Fig. 2(a). The results indicate that for a given boiling curve, at low imposed heat flux the temperature of the heated wall is below the saturated temperature of R-134a and heat transfer in the duct is completely due to the single-phase liquid forced convection. As the imposed heat flux is raised gradually, the

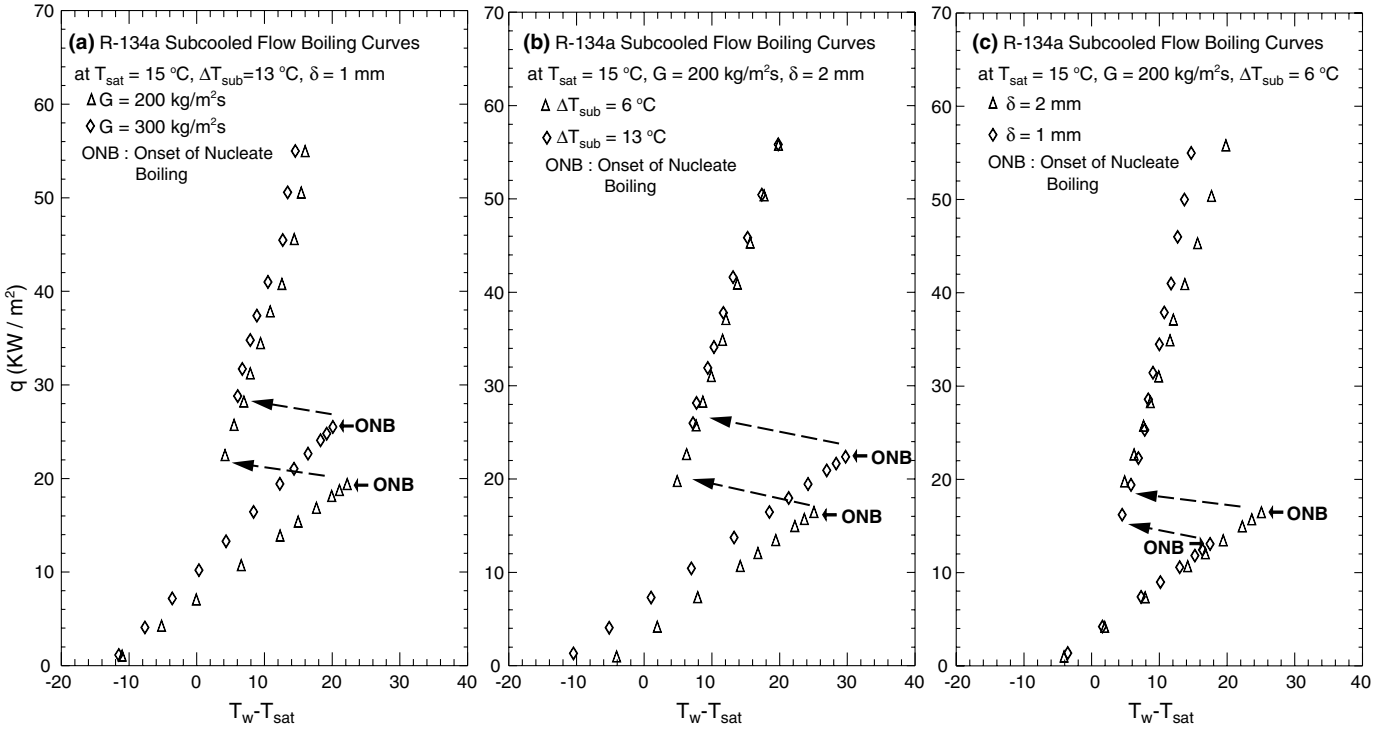

Fig. 2. Subcooled flow boiling curves of R-134a (a) for various refrigerant mass fluxes at $T_{sat} = 15$ °C, $\Delta T_{sub} = 13$ °C and $\delta = 1$ mm, (b) for various inlet subcoolings at $T_{sat} = 15$ °C, $G = 200$ kg/m^2 s and $\delta = 2$ mm, and (c) for various gap sizes at $T_{sat} = 15$ °C, $G = 200$ kg/m^2 s and $\Delta T_{sub} = 6$ °C.

heated wall temperature increases slowly to exceed T_{sat} at a certain q and we have a positive wall superheat ΔT_{sat}. When the positive wall superheat reaches certain critical level, a small increase in q causes boiling bubbles to suddenly appear on the heated wall and the heated wall temperature drops immediately to a noticeable degree. Thus there is a significant temperature undershoot during the onset of nucleate boiling (ONB). Note that the temperature undershoot at ONB can be as high as 18 °C for $G = 200$ kg/m^2 s, $\delta = 1$ mm, $T_{sat} = 15$ °C and $\Delta T_{sub} = 13$ °C (Fig. 2(a)). Note that the refrigerant mass flux to a certain degree affects the magnitude of the temperature undershoot during ONB. Specifically, at a lower mass flux the temperature undershoot is larger. Besides, a slightly higher wall superheat is needed to initiate the nucleate boiling for a lower G. Beyond the ONB a small rise in the wall superheat causes a large increase in the wall heat transfer rate and the slopes of the boiling curves are much steeper than those for the single-phase convection. Checking with the data in Fig. 2(a) further reveals that beyond ONB the refrigerant mass flux exhibits rather slight effects on the boiling curve. But in the single-phase region the heated wall temperature is somewhat affected by the refrigerant mass flux. Note that at a higher mass flux the imposed heat flux needed to initiate ONB is larger.

Next, the effects of the inlet liquid subcooling on the subcooled boiling curves are manifested in Fig. 2(b). The results indicate that at $G = 200$ kg/m^2 s during ONB a substantial increase in the temperature undershoot occurs when the inlet liquid subcooling is raised from 6 °C to 13 °C. Thus a higher wall superheat is needed to initiate the boiling on the heated surface for a higher ΔT_{sub}. We also observed in the experiment that at the higher G of 300 kg/m^2 s the inlet liquid subcooling exhibits only slight influence on the magnitude of the temperature undershoot at ONB. It is also noted from Fig. 2(b) that beyond ONB the boiling curves are not affected to a significant degree by the subcooling in the nucleate boiling region. A similar trend is also noted by Ammerman and You for lower G [22,23]. It is evident that a higher imposed heat flux is needed to initiate boiling on the heated surface for a higher inlet liquid subcooling for a given G. However, in the single-phase region a higher liquid subcooling results in a higher heat transfer from the wall to the refrigerant so that at a given wall superheat the imposed heat flux is significantly higher for a higher liquid inlet subcooling. This reflects the fact that at a given wall superheat the temperature difference between the wall and bulk liquid increases with the inlet subcooling.

Finally, the effects of the duct gap on the boiling curves are shown in Fig. 2(c). Note that a substantial reduction in the temperature undershoot during ONB occurs when the duct gap is reduced from 2 to 1 mm. Thus a lower wall superheat is needed to initiate the boiling on the heated surface for a smaller δ. This mainly results from the fact that for given G, q, T_{sat} and ΔT_{sub} the mass flow rate through the duct is lower for a smaller δ. Thus the axial temperature rise of the refrigerant flow is larger for a smaller δ, which in

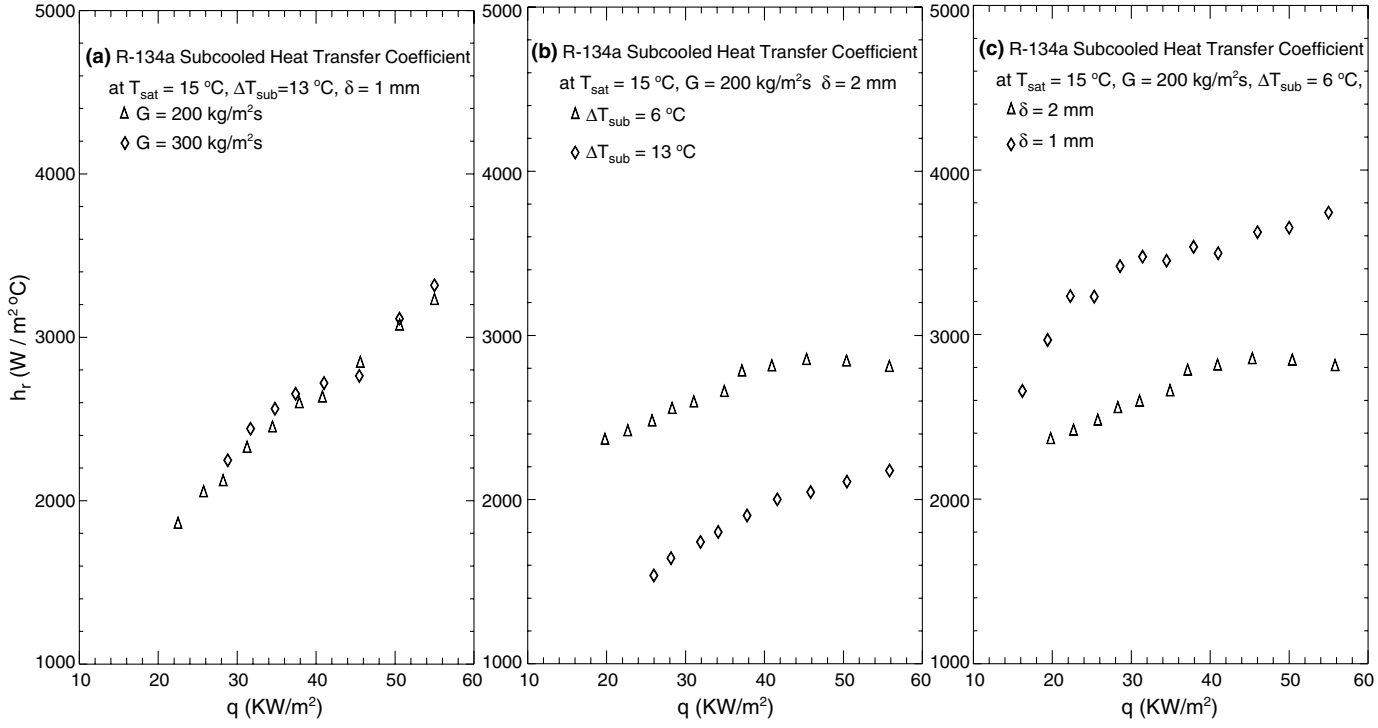

Fig. 3. Subcooled flow boiling heat transfer coefficient of R-134a (a) for various refrigerant mass fluxes at $T_{sat} = 15$ °C, $\Delta T_{sub} = 13$ °C and $\delta = 1$ mm, (b) for various inlet subcoolings at $T_{sat} = 15$ °C, $G = 200$ kg/m^2 s and $\delta = 2$ mm, and (c) for various gap sizes at $T_{sat} = 15$ °C, $G = 200$ kg/m^2 s and $\Delta T_{sub} = 6$ °C.

turn results in a smaller temperature difference between the heated wall and bulk refrigerant flow and hence a lower wall superheat at ONB. It is also noted that the boiling curves are shifted to the left in the nucleate boiling region as the gap size is decreased, indicating that the boiling heat transfer in the duct with a smaller gap is better. Moreover, a lower imposed heat flux is needed to initiate boiling on the heated surface for a duct with a smaller gap for a given G. However, in the single-phase region the effect of δ on the boiling curves is slight. It is also noted in the experiment that the effects of the refrigerant pressure (saturated temperature) on the boiling curves are slight except at low refrigerant mass flux.

4.2. Subcooled flow boiling heat transfer coefficients

The subcooled flow boiling heat transfer coefficients of R-134a measured at the middle axial location ($z = 80$ mm) in the narrow annular duct affected by the three experimental parameters are shown in Fig. 3. The results in Fig. 3(a) indicate that the increase of the subcooled flow boiling heat transfer coefficient with the imposed heat flux is relatively significant at the high inlet liquid subcooling of 13 °C in the narrower duct with $\delta = 1$ mm. Besides, the refrigerant mass flux exhibits a negligible effect on the boiling heat transfer coefficient. However, the boiling heat transfer is much better for a smaller inlet liquid subcooling (Fig. 3(b)). For instance, at $q = 40$ kw/m^2, $T_{sat} = 15$ °C, $G = 200$ kg/m^2 s and $\delta = 2$ mm, h_r for $\Delta T_{sub} = 6$ °C is about 40% higher than that for $\Delta T_{sub} = 13$ °C (Fig. 3(b)). It is of interest to note from the data in Fig. 3(c) that reducing the duct size can effectively enhance the subcooled boiling heat transfer in the duct. For the specific case with $q = 40$ kw/m^2, $T_{sat} = 15$ °C and $\Delta T_{sub} = 6$ °C, h_r for $\delta = 1$ mm is about 30% higher than that for $\delta = 2$ mm (Fig. 3(c)). This is considered to result mainly from the fact that in the narrower duct the radial gradient of the liquid axial velocity is larger, which in turn exerts higher shear force on the bubbles and causes them to depart from the heating surface at a higher rate. This obviously enhances the boiling heat transfer effectively.

4.3. Bubble behavior

When the wall superheat exceeds the incipient boiling temperature, it is noted in the experiment that tiny bubbles form on the active nucleation sites and grow continuously until they depart from the heating surface. At low imposed heat flux the bubble growth and departure are somewhat regular and the bubbles are nearly spherical in shape. The bubble formation, growth and detachment processes in the duct obviously depend on the flow and thermal con-

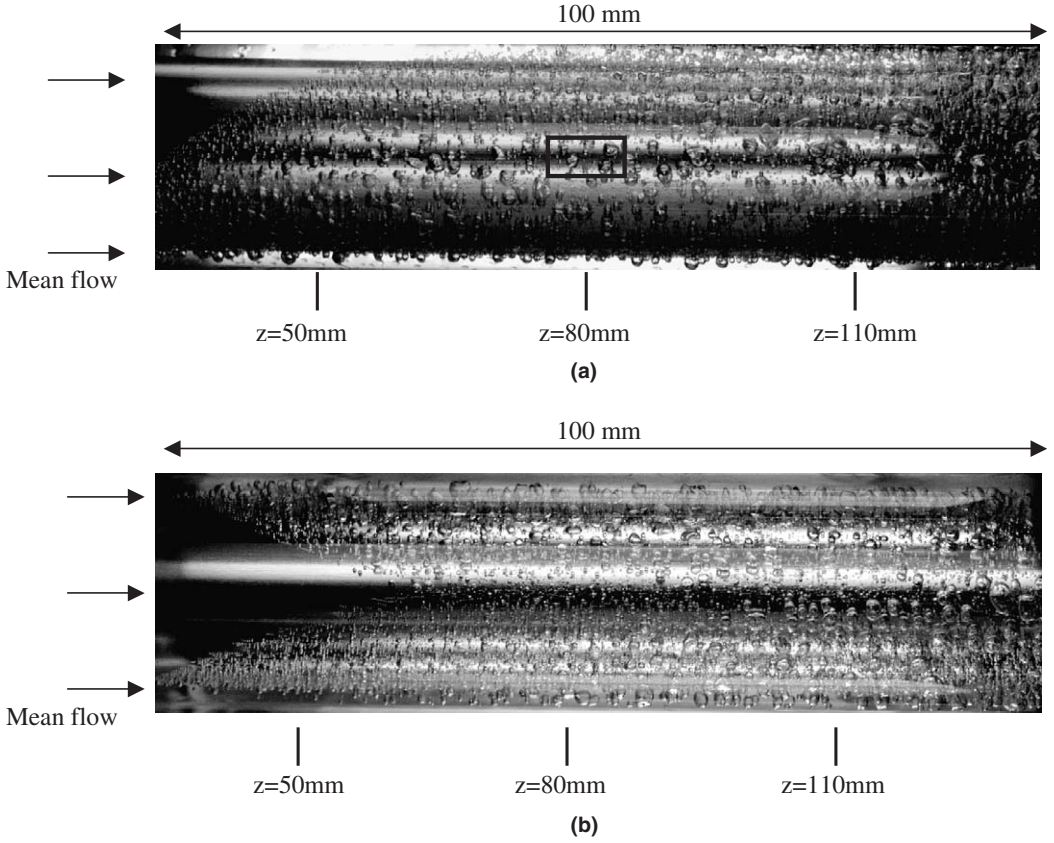

Fig. 4. Photos of boiling flow in the subcooled flow boiling of R-134a in the entire duct at $G = 200$ kg/m^2 s, $T_{sat} = 15$ °C, $\delta = 2$ mm, $\Delta T_{sub} = 6$ °C and $q = 40$ kW/m^2 from (a) side view and (b) top view.

ditions and on the geometry of the active cavities on the heating surface. To illustrate the bubble behavior in the entire duct, photos of the boiling flow from the side and top view covering the whole duct for the case with $G = 200\ \mathrm{kg/m^2\,s}$, $T_{sat} = 15\ ^\circ\mathrm{C}$, $\delta = 2\ \mathrm{mm}$, $\Delta T_{sub} = 6^\circ\mathrm{C}$, and $q = 40\ \mathrm{kW/m^2}$ are shown in Fig. 4. The results clearly indicate that onset of nucleate boiling first appears at the lower part of the heating surface. A longer axial distance is needed for ONB at the upper part of the surface. This is due to the difference in the buoyancy effect in different parts of the duct. More specifically, in the lower portion of the duct the flow is heated from above and hence is thermally stable. This in turn results in a lower convection heat transfer coefficient and obviously the heated surface temperature is higher for a fixed wall heat flux. This higher T_w causes the earlier inception of the bubbles from the surface in the lower portion of the duct. Besides, the bubble motions in the upper and lower portion of the duct are significantly different. On the upper part of the heated surface, bubbles are noted to either lift off directly from the active nucleation sites or slide for a short distance, and then accelerate to a greater speed over that of the surrounding bulk liquid flow. Collision and coalescence of bubbles are insignificant. But in the low portion of the duct, the bubbles departing from the nucleation sites slide circumferentially along the heating surface. Thorncroft and Klausner [24] pointed out that the bubble sliding could enhance the FC-87 flow boiling heat transfer. It is also noted in the present study that the collision and coalescence of bubbles are rather intense except at a low imposed heat flux.

The characteristics of bubbles in the subcooled flow boiling in a small region around the middle axial location ($z = 80\ \mathrm{mm}$) of the annular duct are illustrated in Fig. 5 by showing the side view photos taken from the cases for different imposed heat fluxes, refrigerant mass fluxes, duct sizes and inlet subcoolings. The selected region is marked in Fig. 4(a). Some qualitative features of the bubble motion can be manifested by the flow photos. First of all, the bubbles at the low q of 25 $\mathrm{kw/m^2}$ for the case with $T_{sat} = 15\ ^\circ\mathrm{C}$, $G = 200\ \mathrm{kg/m^2\,s}$, $\delta = 2\ \mathrm{mm}$ and $\Delta T_{sub} = 6\ ^\circ\mathrm{C}$ can be seen from Fig. 5(a). Checking with the video tapes recording the long time bubble motion reveals that the bubbles form and grow at the active nucleation sites while they experience a short period of stationary growth to certain critical sizes. Then the bubbles detach from the heating surface and accelerate in the subcooled liquid. As the imposed heat flux is increased slightly to $q = 35\ \mathrm{kW/m^2}$ (Fig. 5(b)), more bubbles are nucleated on the heating surface and bubbles are occasionally observed to collide and coalesce. The coalescence bubbles are larger and rise faster than the tiny bubbles due to the larger buoyancy force associated with them. As the heat flux is raised to $q = 45\ \mathrm{kW/m^2}$ (Fig. 5(c)), coalescence of the bubbles occurs irregularly. In fact, the large coalescence bubbles are highly deformed. At even higher heat fluxes the bubble nucleation density becomes too large to visually distinguish the individual nucleation sites. In general, increasing the imposed heat flux directly provides more energy to the cavities and more cavities on the heating surface can be activated. Besides, the bubble departure frequency is also found to increase substantially with the imposed heat flux. Moreover, the bubble departure diameter increases slightly with the imposed heat flux due to the resulting higher wall superheat. Note that the buoyancy and shear force cause the bubbles to lift off and depart from the heating surface, but the surface tension tends to keep the bubbles to stay on the heating surface.

Next, Fig. 5(d)–(f) shows the bubble characteristics around the middle axial location affected by the refrigerant mass flux by presenting the photos for the higher G of 300 $\mathrm{kg/m^2\,s}$ but at the same q, T_{sat}, δ and ΔT_{sub} as that for Fig. 5(a)–(c). A close inspection of the corresponding photos and video tapes at different mass fluxes reveals that at a higher G the higher liquid speed can condense the bubbles intensively in the early stage of the bubble growth, resulting in a lower bubble departure frequency and smaller bubble departure diameter. Thus the partial nucleate boiling dominates in the flow at a high G and low q. But the higher liquid speed for a higher G can sweep the bubbles away from the cavities in an easier way resulting in a higher bubble departure frequency. Besides, at a higher G the liquid temperature is lower for a given imposed heat flux at a given ΔT_{sub}. Hence less bubble nucleation is activated on the heated surface and the bubble nucleation density is lower.

Then, the bubble characteristics affected by the duct size are revealed by comparing the photos in Fig. 5(a)–(c) for $\delta = 2\ \mathrm{mm}$ with Fig. 5(g)–(i) for $\delta = 1\ \mathrm{mm}$ at $q = 25$–$45\ \mathrm{kW/m^2}$, $G = 200\ \mathrm{kg/m^2\,s}$, $T_{sat} = 15\ ^\circ\mathrm{C}$ and $\Delta T_{sub} = 6\ ^\circ\mathrm{C}$. Due to the space limitation in the narrow duct for $\delta = 1\ \mathrm{mm}$ bubbles are squeezed and deformed to some degree. Besides, at $\delta = 1\ \mathrm{mm}$ more large bubbles, which result from the coalescence of the small bubbles, are found to slide along the heated surface for some distance before they detach from the heated surface. Moreover, these sliding bubbles have more time to absorb the thermal energy from the heated surface while sliding along the surface and therefore grow up to become bigger. Many large and deformed bubbles are noted to float in the upper part of the channel at high heat flux. As mentioned earlier, in the smaller duct the shear force in the subcooled liquid flow is stronger to sweep the growing bubbles more quickly away from the heating surface, which increases the bubble departing frequency.

Finally, the effects of the inlet liquid subcooling on the bubble characteristics are illustrated by comparing the photos shown in Fig. 5(j)–(l) for $\Delta T_{sub} = 13\ ^\circ\mathrm{C}$ with Fig. 5(a)–(c) for $\Delta T_{sub} = 6\ ^\circ\mathrm{C}$ at $q = 25$–$45\ \mathrm{kW/m^2}$, $G = 200\ \mathrm{kg/m^2\,s}$, $\delta = 2\ \mathrm{mm}$ and $T_{sat} = 15\ ^\circ\mathrm{C}$. In general, bubbles are larger at a lower subcooling. The larger bubbles are the consequences of the weaker vapor condensation and more bubble coalescence at a lower inlet subcooling. In addition, an increase in the inlet subcooling reduces the bubble departure frequency. This is due to the fact that

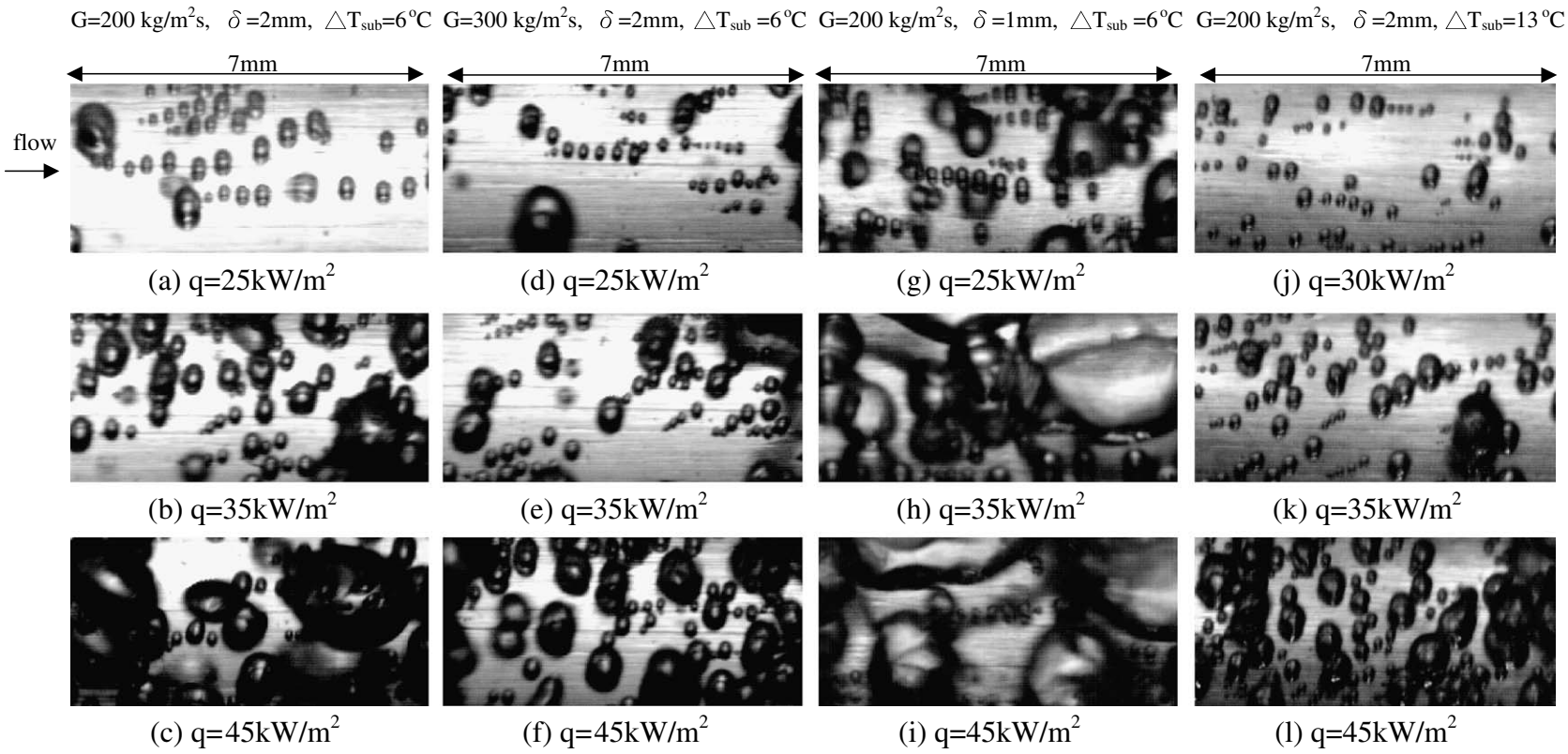

Fig. 5. Photos of bubbles in the subcooled flow boiling of R-134a in a small region around middle axial location for $T_{sat} = 15$ °C for various imposed heat flux, mass fluxes, gap sizes and inlet liquid subcoolings.

at a higher inlet liquid subcooling the temperature of the subcooled liquid–vapor interface is relatively low compared to the hot heated surface. Hence at the same imposed heat flux, the wall superheat is not high enough to sustain the continuing growth of the bubbles when the inlet liquid subcooling is high. Besides, the active nucleation sites decrease at increasing inlet subcooling. The above results clearly reveal the significant influences of the liquid inlet subcooling on the bubble characteristics.

To quantify the bubble characteristics, we move further to estimate the mean bubble departure diameter and frequency and the mean active nucleation site density on the heating surface by carefully tracing the motion of the bubbles from the images of the boiling flow stored in the video tapes. These quantitative data are examined in the following. The effects of the refrigerant mass flux, inlet subcooling, and duct size on the bubble departure diameter for the subcooled flow boiling of R-134a in the small region at the middle axial location ($z = 80$ mm) of the annular duct are shown in Fig. 6. First, the data given in Fig. 6(a) indicate that the average bubble departure diameter is somewhat larger for a smaller refrigerant mass flux. Note that the effect of the refrigerant mass flux on the bubble departure diameter is more pronounced at low imposed heat flux. Next, it is observed from Fig. 6(b) that the average bubble departure diameter is noticeably larger for a smaller liquid subcooling especially at low imposed heat flux. Finally, the results shown in Fig. 6(c) manifest that the average departing bubbles are larger in the smaller duct. According to the present experimental data, the effects of T_{sat} on d_p are slight.

How the experimental parameters affect the mean bubble departure frequency for the subcooled flow boiling of R-134a are illustrated in Fig. 7. First, the data shown in Fig. 7(a) indicate that the average bubble departure frequency is higher for a larger refrigerant mass flux especially at high imposed heat flux. At $q = 40$ kw/m^2, $T_{sat} = 15$ °C, $\Delta T_{sub} = 6$ °C and $\delta = 1$ mm, the average bubble departure frequency for $G = 300$ kg/m^2 s is about 44% higher than that for $G = 200$ kg/m^2 s (Fig. 7(a)). Next, it is noted from Fig. 7(b) that the average bubble departure frequency is somewhat higher for a smaller liquid subcooling. Fig. 7(c) shows that the average bubble departure frequency is higher for the smaller duct. The effect is more prominent at a high imposed heat flux. It is also noted in the experiment that the refrigerant saturated temperature exhibits rather slight effects on the bubble departure frequency.

The mean number density of the active bubble nucleation sites affected by the experimental parameters in the subcooled flow boiling of R-134a is shown in Fig. 8. The results in Fig. 8(a) indicate that the average active nucleation site density is significantly higher for a smaller refrigerant mass flux. Next, Fig. 8(b) shows that the average active nucleation site density is somewhat higher for a smaller liquid subcooling. As an example, at

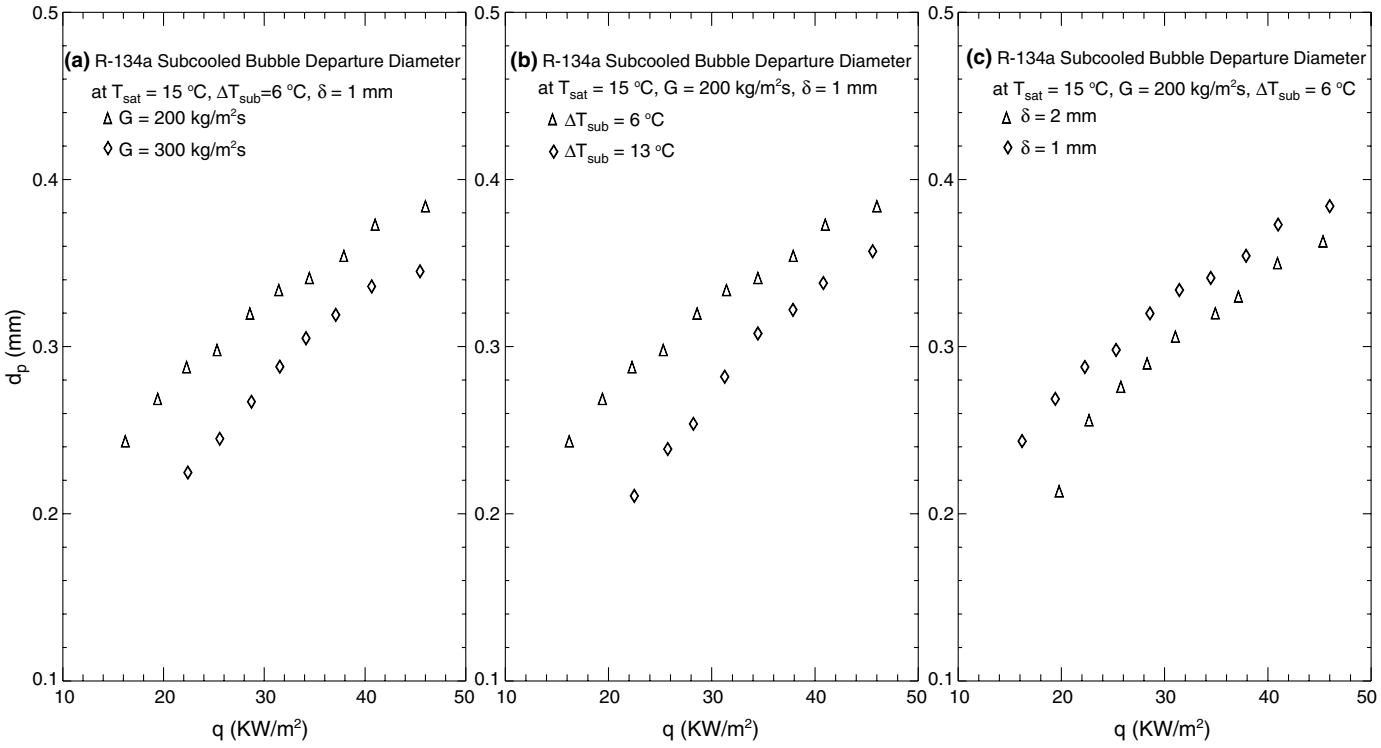

Fig. 6. Mean bubble departure diameter for subcooled flow boiling of R-134a (a) for various refrigerant mass fluxes at $T_{sat} = 15$ °C, $\Delta T_{sub} = 6$ °C and $\delta = 1$ mm, (b) for various inlet subcoolings at $T_{sat} = 15$ °C, $G = 200$ kg/m^2 s and $\delta = 1$ mm, and (c) for various gap sizes at $T_{sat} = 15$ °C, $G = 200$ kg/m^2 s and $\Delta T_{sub} = 6$ °C.

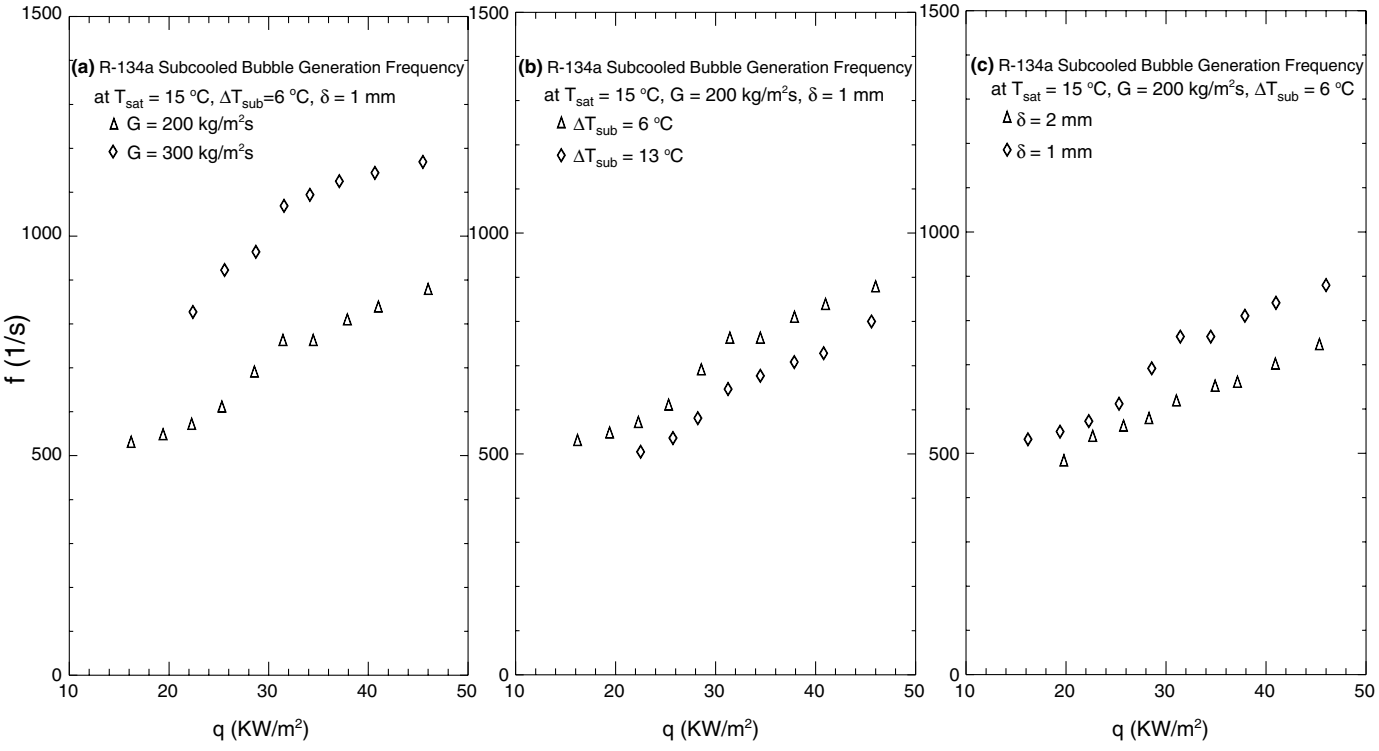

Fig. 7. Mean bubble departure frequency for subcooled flow boiling of R-134a (a) for various refrigerant mass fluxes at $T_{sat} = 15$ °C, $\Delta T_{sub} = 6$ °C and $\delta = 1$ mm, (b) for various inlet subcoolings at $T_{sat} = 15$ °C, $G = 200$ kg/m^2 s and $\delta = 1$ mm, and (c) for various gap sizes at $T_{sat} = 15$ °C, $G = 200$ kg/m^2 s and $\Delta T_{sub} = 6$ °C.

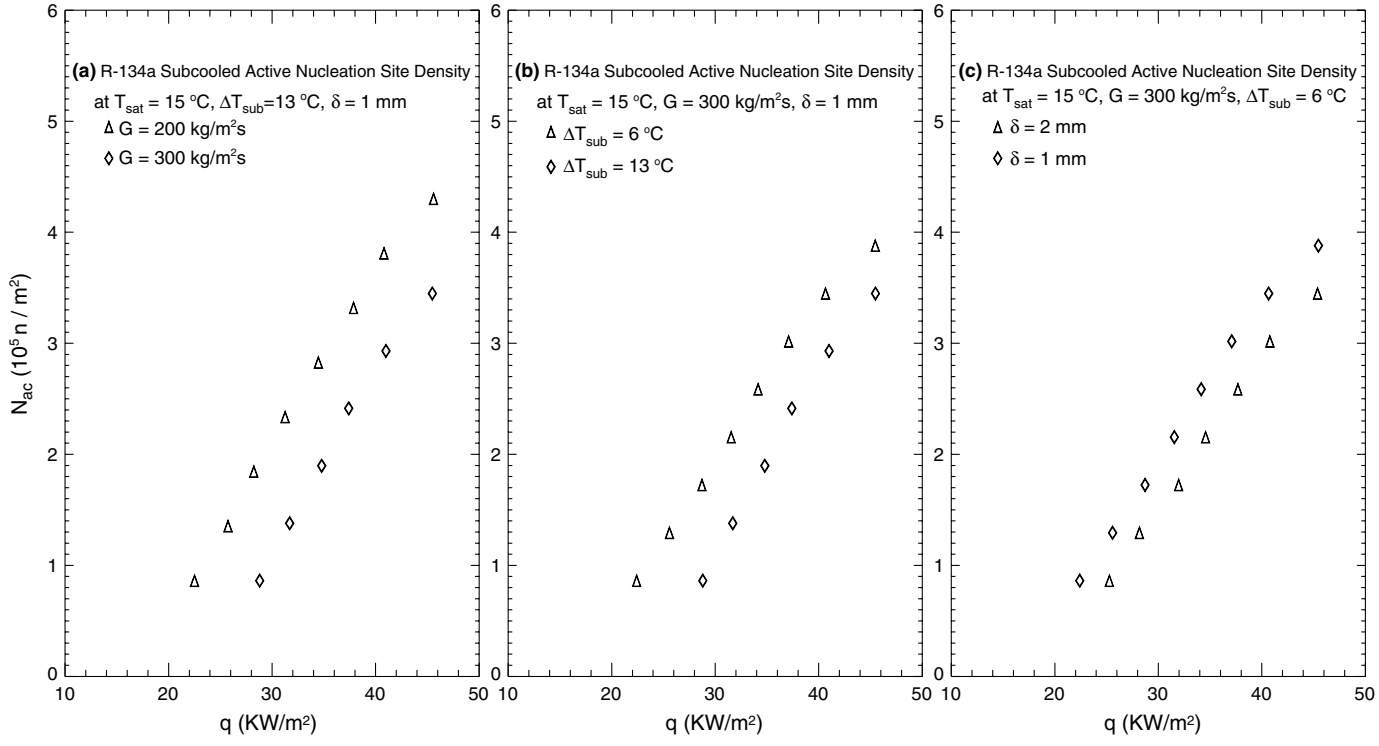

Fig. 8. Mean active nucleation site density for subcooled flow boiling of R-134a (a) for various refrigerant mass fluxes at $T_{sat} = 15$ °C, $\Delta T_{sub} = 13$ °C and $\delta = 1$ mm, (b) for various inlet subcoolings at $T_{sat} = 15$ °C, $G = 300$ kg/m^2 s and $\delta = 1$ mm, and (c) for various gap sizes at $T_{sat} = 15$ °C, $G = 300$ kg/m^2 s and $\Delta T_{sub} = 6$ °C.

$q = 40$ kw/m^2, $T_{sat} = 15$ °C, $G = 300$ kg/m^2 s and $\delta = 1$ mm, the average active nucleation site density for $\Delta T_{sub} = 6$ °C is about 21% higher than that for $\Delta T_{sub} = 13$ °C. Finally, the data in Fig. 8(c) manifest that the average active nucleation site density is higher to some degree in a smaller duct especially at a high imposed heat flux and a lower ΔT_{sub}. The refrigerant saturated temperature is also found to have negligible effects on the active bubble nucleation site density.

4.4. Correlation equations

An empirical equation to correlate the present data of the heat transfer coefficient in the subcooled flow boiling of R-134a in the horizontal annular duct with a narrow gap is proposed here. The total heat flux input to the boiling flow q_t is considered to consist of two parts: one resulting from the bubble nucleation q_b and another due to the single-phase liquid forced convection q_c. Thus

$$q_t = q_b + q_c \tag{2}$$

Here q_b and q_c can be respectively calculated from the quantitative data for the bubble characteristics presented above and single-phase forced convection as

$$q_b = \rho_g \cdot V_g \cdot f \cdot N_{ac} \cdot i_{fg} \tag{3}$$

and

$$q_c = E \cdot h_{1\phi}(T_w - T_r) \tag{4}$$

Note that in the above equation an enhancement factor E is added to q_c to account for the agitating motion of the bubbles which can enhance the single-phase convection heat transfer. Empirically, E and $h_{1\phi}$ can be correlated as

$$E = 20N_{conf}^{0.65} \cdot Fr_l^{-0.75} \cdot (1 - 250Bo)^{3.6} \tag{5}$$

and

$$h_{1\phi} = Nu \cdot k_l / D_h \tag{6}$$

Note that Nu is estimated from the Gnielinski correlation,

$$Nu = \frac{(f_f/2)(Re_l - 1000)Pr_l}{1.07 + 12.7\sqrt{f_f/2}(Pr^{2/3} - 1)} \tag{7}$$

Here f_f is the friction factor and is correlated as

$$f_f = (1.58 \ln Re_l - 3.28)^{-2} \tag{8}$$

where ρ_g is the vapor density, V_g is the vapor volume of the departing bubble which is equal to $\frac{4\pi}{3}\left(\frac{d_p}{2}\right)^3$, f is bubble departure frequency, N_{ac} is the active nucleation site density, i_{fg} is the enthalpy of vaporization. Because the experimental Re_l ranges from 1600 to 5000, we use the Gnielinski correlation to evaluate the single-phase forced convection heat transfer. At a higher imposed heat flux for $q > 40$ kW/m^2, it is difficult to distinguish the individual bubbles and the above correlations do not apply.

To enable the usage of the above correlation for computing the flow boiling heat transfer, the mean bubble size and departure frequency and the active nucleation site density on the heating surface need to be correlated in advance. The average bubble departure diameter in the subcooled flow boiling of R-134a in the narrow annular duct estimated from the present flow visualization can be correlated as

$$D_p = \frac{d_p}{\sqrt{\sigma/g \cdot \Delta\rho}} = \frac{315 \cdot N_{conf}\left(\rho_l/\rho_g\right)^{0.333}}{Re_l^{0.5} \cdot \left[Ja + \frac{165 \cdot \left(\rho_l/\rho_g\right)^{1.333}}{Bo^{0.5} \cdot Re^{1.4}}\right]} \tag{9}$$

Fig. 9 shows that almost all the present experimental data for d_p fall within ±25% of the above correlation and the mean absolute error is 14.3%. Besides, an empirical equation is proposed for the product of the mean bubble departure diameter and frequency as

$$F_d = \frac{f \cdot d_p}{\mu_l/(\rho_l D_h)} = 1642 \cdot Re_l^{0.887} \cdot Ja^{-0.05} \cdot Bo^{0.887} \cdot N_{conf}^{0.01} \tag{10}$$

Note that more than 90% of the experimental data for $f \cdot d_p$ collected in this study can be correlated within ±25% by Eq. (10) and the mean absolute error is 16.2% (Fig. 10). Finally, we propose an empirical correlation for the average active nucleation site density in the subcooled flow boiling of R-134a as

$$N_{ac} = 80352 + 8034 \cdot \Delta T_{sat}^{1.67} N_{conf}^{0.51} \tag{11}$$

Fig. 11 shows that the present experimental data fall within ±30% of the above correlation and the mean absolute error is 22.8%.

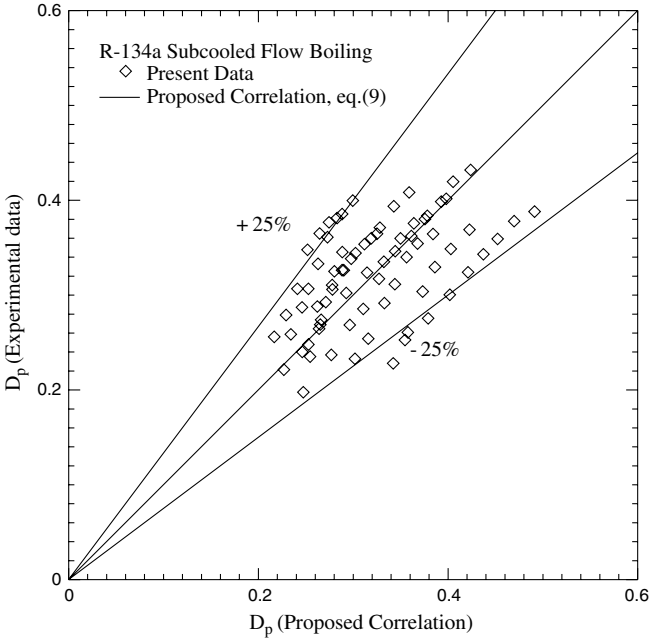

Fig. 9. Comparison of the measured data for mean bubble departure diameter in the subcooled flow boiling of R-134a with the proposed correlation.

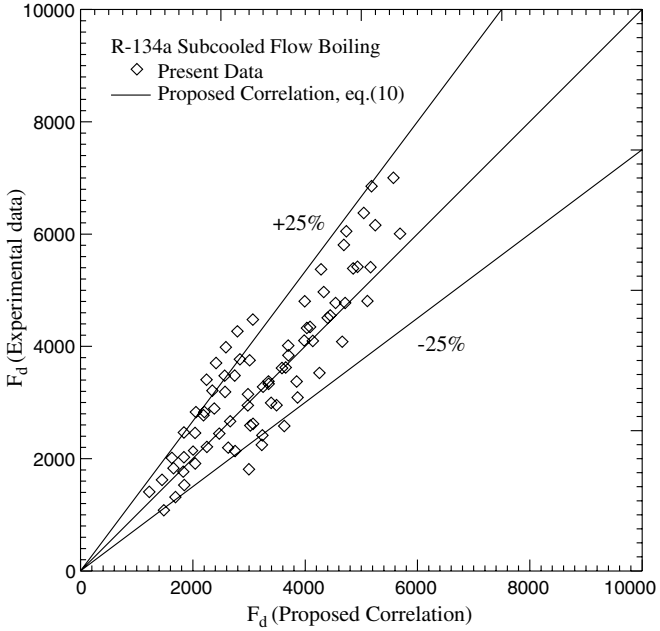

Fig. 10. Comparison of the measured data for mean bubble departure frequency in the subcooled flow boiling of R-134a with the proposed correlation.

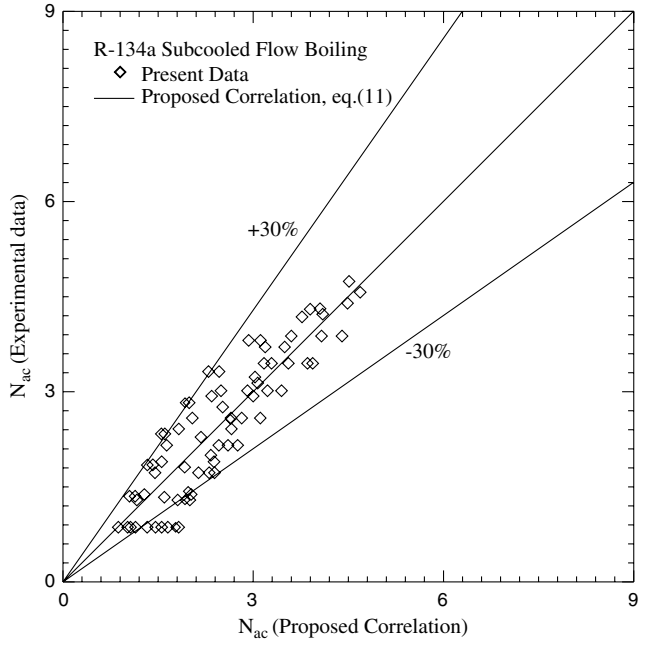

Fig. 11. Comparison of the measured data for mean active nucleation site density in the subcooled flow boiling of R-134a with the proposed correlation.

When the correlations for d_p, f, and N_{ac} given in Eqs. (9)–(11) are combined with Eqs. (2)–(8) for q_t, more than 90% of the heat transfer data measured in the present study fall within ±30% of the correlation proposed here with a mean deviation of 14.8% (Fig. 12).

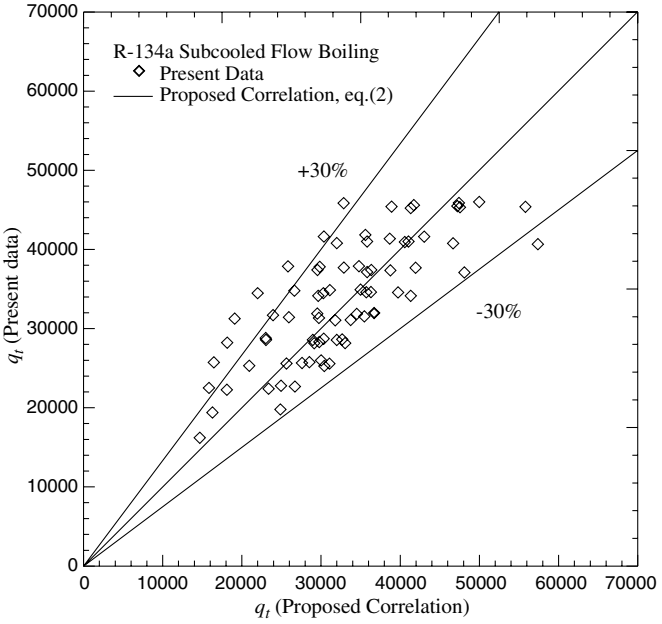

Fig. 12. Comparison of the measured data for heat transfer coefficient in the subcooled flow boiling of R-134a with the proposed correlation.

5. Concluding remarks

The experimental heat transfer data and associated bubble behavior for the subcooled flow boiling of R-134a in the horizontal narrow annular ducts have been presented here. The effects of the imposed heat flux, refrigerant mass flux, inlet subcooling, and duct size on the subcooled flow boiling heat transfer coefficient and associated bubble characteristics have been examined in detail. In addition, empirical equations to correlate the measured heat transfer data and bubble characteristics are provided. The major results obtained in the present study can be summarized in the following.

(1) The temperature overshoot at ONB is significant for the subcooled flow boiling of R-134a in the narrow annular duct.
(2) The R-134a subcooled flow boiling heat transfer coefficient increases with a decrease in the duct size, but decreases with an increase in the inlet subcooling. Besides, raising the imposed heat flux can cause a significant increase in the boiling heat transfer coefficients. However, the effects of the refrigerant mass flux and saturated temperature on the boiling heat transfer coefficient are small.
(3) Correlation equations are provided for the boiling heat transfer coefficient, bubble departure diameter, bubble departure frequency and active nucleation site density in the R-134a subcooled flow boiling.
(4) Visualization of the bubble motion in the boiling flow reveals that the bubbles are suppressed to become smaller and less dense by raising the refrigerant mass flux and inlet subcooling. Moreover, raising the

imposed heat flux produces positive effects on the bubble population, coalescence and departure frequency.

Acknowledgements

The financial support of this study by the Engineering Division of National Science Council of Taiwan, ROC through the contract NSC 93-2212-E-009-05 is greatly appreciated.

References

[1] C. Vlasie, H. Macchi, J. Guilpart, B. Agostini, Flow boiling in small diameter channels, International Journal of Refrigeration 27 (2004) 191–201.
[2] B. Watel, Review of saturated flow boiling in small passages of compact heat exchangers, International Journal of Thermal Science 42 (2003) 107–140.
[3] W. Yu, D.M. France, M.W. Wambsganss, J.R. Hull, Two-phase pressure drop, boiling heat transfer, and critical heat flux to water in a small-diameter horizontal tube, International Journal of Multiphase Flow 28 (6) (2002) 927–941.
[4] Y. Fujita, Y. Yang, N. Fujita, Flow boiling heat transfer and pressure drop in uniformly heated small tubes, Proceedings of the Twelfth International Heat Transfer Conference 3 (2002) 743–748.
[5] T.N. Tran, M.W. Wambsganss, D.M. France, Small circular- and rectangular-channel boiling with two refrigerants, International Journal of Multiphase Flow 22 (3) (1996) 485–498.
[6] Z.Y. Bao, D.F. Fletcher, B.S. Haynes, Flow boiling heat transfer of Freon R11 and HCFC123 in narrow passages, International Journal of Heat and Mass Transfer 43 (18) (2000) 3347–3358.
[7] B.S. Haynes, D.F. Fletcher, Subcooled flow boiling heat transfer in narrow passages, International Journal of Heat and Mass Transfer 46 (2003) 3673–3682.
[8] S. Su, S. Huang, X. Wang, Study of boiling incipience and heat transfer enhancement on forced flow through narrow channels, International Journal of Multiphase Flow 31 (2005) 253–260.
[9] M. Piasecka, S. Hozejowska, M.E. Poniewski, Experimental evaluation of flow boiling incipience of subcooled fluid in a narrow channel, International Journal of Heat and Fluid Flow 25 (2004) 159–172.
[10] V.V. Kuznetsov, O.S. Kim, A.S. Shamirzaev, Flow boiling heat transfer in an annular channel with a small gap, Russian Journal of Thermophysics 9 (4) (1999) 273–283.
[11] S. Qiu, M. Takahashi, G.H. Su, D. Jia, Experimental study on heat transfer of singlephase flow and boiling twophase in vertical narrow annuli, Proc of 10th International Conference on Nuclear Engineering 3 (2002) 319–324.
[12] M. Aritomi, T. Miyata, M. Horiguchi, A. Sudi, Thermo-hydraulics of boiling two-phase flow in high conversion light water reactors (thermo-hydraulics at low velocities), International Journal of Multiphase Flow 19 (1) (1993) 51–63.
[13] C.H. Sheng, B. Palm, The visualization of boiling in small diameter tubes, in: Proc. of International Conference on Heat Transfer and Transport Phenomena in Microscale, Banff, Canada, October 15–20, 2000, pp. 204–208.
[14] P.C. Lee, F.G. Tseng, C. Pan, Bubble dynamics in microchannels. Part I: single microchannel, International Journal of Heat and Mass Transfer 47 (2004) 5575–5589.
[15] C. Bang, W.P. Baek, and S.H. Chang, A digital photographic study on nucleate boiling in subcooled flow for water and refrigerant 134a fluids, in: Proc. of 10th International Conference on Nuclear Engineering, Arlington, VA, April 14–18, 2002, vol. 3, pp. 155–162.
[16] R. Situ, Y. Mi, M. Ishii, M. Mori, Photographic study of bubble behaviors in forced convection subcooled boiling, International Journal of Heat and Mass Transfer 47 (2004) 3659–3667.
[17] C.P. Yin, Y.Y. Yan, T.F. Lin, B.C. Yang, Subcooled flow boiling heat transfer of R-134a and associated bubble characteristics in a horizontal annular channel, International Journal of Heat and Mass Transfer 43 (2000) 1885–1896.
[18] G.E. Thorncroft, J.F. Klausner, R. Mei, An experimental investigation of bubble growth and detachment in vertical upflow and downflow boiling, International Journal of Heat and Mass Transfer 41 (23) (1998) 3857–3871.
[19] O. Zeitoun, M. Shoukri, Bubble behavior and mean diameter in subcooled flow boiling, ASME Journal of Heat Transfer 118 (1996) 110–116.
[20] Y.M. Lie, T.F. Lin, Saturated flow boiling heat transfer and associated bubble characteristics of R-134a in a narrow annular duct, International Journal of Heat and Mass Transfer 48 (25–26) (2005) 5602–5615.
[21] S.J. Kline, F.A. McClintock, Describing uncertainties in single-sample experiments, Mechanical Engineering 75 (1) (1953) 3–12.
[22] C.N. Ammerman, S.M. You, Enhancing small-channel convective boiling performance using a microporous surface coating, ASME Journal of Heat Transfer 123 (5) (2001) 976–983.
[23] C.N. Ammerman, S.M. You, Enhanced convective boiling of FC-87 in small, rectangular, horizontal channels: heat transfer coefficient and CHF, ASME HTD 357 (4) (1998) 225–231.
[24] G.E. Thorncroft, J.F. Klausner, The influence of vapor bubble sliding on forced convection boiling heat transfer, ASME Journal of Heat Transfer 121 (1999) 73–79.